

Effect of Ferromagnetic Induced Inhomogeneity in Excess Conductivity of $\text{YBa}_2\text{Cu}_3\text{O}_{7-\delta+x}\text{CoFe}_2\text{O}_4$ Composite

Sahoo M* and Behera D

Department of Physics, National Institute of Technology, Rourkela 769008, India

Abstract

Dimensional fluctuations of superconducting order parameters in $\text{YBa}_2\text{Cu}_3\text{O}_{7-\delta+x}\text{CoFe}_2\text{O}_4$ ($x = 0.0, 0.1, 0.2,$ and 0.3 wt%) has been analyzed. SEM micro-graphs reveal the reduced grain size with the incorporation of ferromagnetic CoFe_2O_4 particles in the YBCO matrix. With the increase of CoFe_2O_4 wt% it is found that the superconducting transition temperatures (T_c) determined from standard four-probe method decreases and dropped sharply with higher wt.% addition of CoFe_2O_4 . Excess conductivity fluctuation analysis using Aslamazov-Larkin (AL) model fitting reveals transition of two dominant regions (2D and 3D) above T_c . 2D to 3D crossover temperature i.e. Lawrence-Doniach temperature (T_{LD}) that demarcates dimensional nature of fluctuation inside the grains is influenced by CoFe_2O_4 incorporation in YBCO matrix. The decrease in T_{LD} in the mean field region has been observed as a consequent dominance of 3D region with increase in wt% of CoFe_2O_4 in the composite. The decrease in zero-resistance critical temperature (T_{c0}) and increase in transition width (ΔT) signifies the degradation of inter-grain weak links.

Keywords: YBCO; Ferromagnetic CoFe_2O_4 ; Excess conductivity; AL model; Current percolation

Introduction

The study of thermodynamic fluctuation is distinctly marked in the mixed state of type II superconductors after the discovery of High Temperature Superconductors (HTSC) in 1986. The effects of thermodynamic fluctuations in HTSC are prominently well above the mean field transition temperature (T_c) [1] due to their short coherence length, high transition temperature and high anisotropy property of the material. The study of the transport properties especially in the region of T_c is a tool for studying the characteristics of the superconducting phase. Among those of interest is the excess conductivity or para-conductivity above T_c . This conductivity is related to the thermodynamical fluctuations due to the presence of thermal fluctuations of Cooper pairs above T_c [2]. The chosen material $\text{YBa}_2\text{Cu}_3\text{O}_{7-\delta}$ has several advantages over other ceramic superconductors. This is the most stable compound with a T_c above 77 K. It has neither toxic nor volatile elements. It is easy to make single-phase of YBCO and less anisotropic than other HTS materials. It possesses high J_c at higher magnetic field than other HTSC, YBCO is one of the materials being considered as potential candidates for applications such as microwave devices, power transmission tape, and delay lines. This is the most useful material for conductor applications because of its high irreversibility field. The capability to transport electric current without any energetic dissipation, together with its low thermal conductivity, suggest the application of HTSC for high current transport to low temperature SC devices such as magnets [3]. It is also used in fault current limiters which operate at 77K, maglev trains, SQUIDS and in computers [4]. Among the different models proposed to explain the fluctuation effects, the most appreciated ones are that of Aslamazov and Larkin [5], Maki-Thompson (MT) and Lawrence-Doniach (LD) [6] for the two-dimensional layered superconductors. Several models [7,8] have been proposed to describe the complete shape of resistive transition in the presence of magnetic fields.

Superconductor composite materials have significantly improved electrical and magnetic properties. The generated defects such as twins and inhomogeneous micro-defects can act as additional pinning centers, resulting in an increase of the critical current density at higher magnetic fields [9-12]. The artificial pinning centers besides the above defects-induced pinning centers are more efficient to enhance

current density. The composite decreases the number of weak-links and significant enhancement of the superconducting critical current density J_c in applied magnetic field has been reported [13]. The practical introduction of effective flux pinning sites into HTSC is of paramount importance for their widespread application. The search for suitable process for the generation of nanoscale defects to act as core pinning sites in the superconductor matrix has been highly fruitful, yielding improvements in the critical current density [4]. Flux pinning by magnetic materials may be expected to provide an additional contribution to the pinning potential through the magnetic interaction between the material and the flux vortices, supplementing the core pinning that results from the inclusion of non-superconducting material within the superconducting matrix. Till now, attempts have been made with Fe, Co and Ni, as well as with simple metal oxides such as Fe_2O_3 [14] but all have resulted in a detrimental effect on the superconducting properties through cross-contamination into the YBCO matrix and a subsequent suppression of T_c . In this paper attempts have been made to analyze the effect of ferromagnetic inclusions to YBCO matrix on structural and electrical transport properties around the transition temperature.

Experimental

$\text{YBa}_2\text{Cu}_3\text{O}_{7-\delta}$ superconductor powder was synthesized from precursor powders of Y_2O_3 , BaCO_3 , and CuO . A stoichiometric amount of the cationic ratio of Y: Ba: Cu = 1:2:3 was stirred in 2-Methyl ethanol and mixed well for 12 hrs. This solution was dried and evaporated at 70-80°C until well mixed powders were obtained. Then, the powders were ground for 2 hrs, and calcined at 900°C for 12 hrs. The pellets were made

*Corresponding author: Sahoo M, Department of Physics, National Institute of Technology, Rourkela 769008, India, Tel: +916612462724; Fax: +916612462999; E-mail: sahoomousumi@gmail.com

Received October 02, 2012; Accepted October 23, 2012; Published October 30, 2012

Citation: Sahoo M, Behera D (2012) Effect of Ferromagnetic Induced Inhomogeneity in Excess Conductivity of $\text{YBa}_2\text{Cu}_3\text{O}_{7-\delta+x}\text{CoFe}_2\text{O}_4$ Composite. J Material Sci Eng 1:115. doi:10.4172/2169-0022.1000115

Copyright: © 2012 Sahoo M, et al. This is an open-access article distributed under the terms of the Creative Commons Attribution License, which permits unrestricted use, distribution, and reproduction in any medium, provided the original author and source are credited.

from the calcined powders, sintered at 920°C for 12 hours and annealed at 500°C for eight hours for oxygen uptake. A series of polycrystalline composite samples of $(1-x)\text{YBCO}_{7-\delta+x}\text{CoFe}_2\text{O}_4$ (where $x = 0.0, 0.1, 0.2, 0.3$ wt%) were ground and pressed into pellets. The composite pellets were sintered at 920°C for 12 hours and then cooled to 500°C where they were kept for five hours in an oxygen atmosphere for oxygen intake. XRD and SEM characterization was done for structural and micro structural analysis. Temperature dependent resistivity $\rho(T)$ was measured using standard four-probe technique with a Nanovoltmeter (Keithley-2182A) and constant current source (Keithley 6221), with the voltage resolution of 10^{-8} V of the Nanovoltmeter, a constant current source of one mA flowing through the samples. A closed cycle Helium refrigerators (JANIS) and a temperature controller (Lakeshore 332) having a temperature resolution of ± 0.1 K were used for temperature variation. Computer controlled data acquisition system was used with Lab view program.

Results and Discussion

XRD analysis

Figure 1 shows the X-ray diffraction patterns of the $\text{YBa}_2\text{Cu}_3\text{O}_{7-\delta}/x\text{CoFe}_2\text{O}_4$ composite samples. The diffraction pattern of the composite samples is indexed using Chek Cell software and the results are found to be in orthorhombic phase with a space group P_{mmm} , with some CoFe_2O_4 peaks and without any noticeable impurity peaks. The presence of (311), (400), (422) peaks of CFO in 0.1wt.% and (333), (440) peaks of CFO in 0.2 wt% in the 2θ range of 35.51°-62.65° give an evidence for the formation of CFO crystallites within the pristine YBCO sample. The Intensity at (010), (005) and (020) planes of YBCO increases gradually with an increase in wt% of CFO, which signifies that more no. of diffraction are coming from these planes.

From the table 1 data it is clear that there is no significant change in 'b' parameter except 0.1 wt% added sample. The length of 'a' parameter is greater in the composite samples as compared to that of pure samples except for 0.1 wt% composite. The similar case was also happening in the case of 'c' parameter and for the volume of the crystallites. This elongation is expected due to the strain effect i.e. the non-uniform elastic distortions of the crystal lattice at the atomic level imposed by the magnetic inhomogeneity on YBCO matrix. The orthorhombic distortion remains almost constant in all the samples except 0.1 wt% added sample. It is highest for this sample. This value is more means oxygen ordering more. Superconductivity of YBCO is associated not only with the oxygen content but also with the ordering of the oxygen atoms and oxygen vacancies in the Cu-O basal plane. The complete ordering is reflected in rows of empty O(5) and filled oxygen sites O(1). This asymmetric distribution of oxygen leads to an orthorhombic distortion ($b-a/b+a$), that is a measure of ordering. The big difference between b and a corresponds to the higher ordering degree [15]. It can also be seen that the lattice parameter c is smaller for the sample with higher ordering. The smaller c value could be responsible for a better interlayer exchange and consequently, could give better superconducting properties [16]. The oxygen stoichiometry value is calculated from the relation $7-\delta=75.250-5.856c$, where c is the c-axis lattice parameter [17]. Oxygen value is more in 0.1 wt% sample where the orthorhombic distortion more.

Microstructural and EDX analysis

The micro-structure characterization i.e. grain size distribution of the composites is shown in figure 2. From SEM images it is observed that both YBCO and CoFe_2O_4 exhibits randomly oriented grains.

With the ferromagnetic CoFe_2O_4 addition, two changes on the micro-structure have been observed. Firstly, the grain becomes elongated and size gradually reduced. Decrease in grain size indicates that the strength and hardness of the sample increase gradually. Secondly, CoFe_2O_4 particles are observed sticking to the surface filling up cracks and voids, which is evident from figure 2 (c,e). Extra deposition of CoFe_2O_4 is observed between grains for 0.3 wt. % (Figure 2e) which may be accounted to excess addition of CoFe_2O_4 . White patches of CoFe_2O_4 are also observed in figure 2e. However, in granular HTSCs in the superconducting state (below T_c), transport properties are mainly controlled by the grain boundary micro-structure, unlike T_c , which is determined by the crystal structure and oxygen content [18]. The EDX graphs show all the compositional elements in proper stoichiometric amount.

Temperature dependence of resistivity analysis

Measurements of the resistivity dependence of temperature for different samples with various amounts of CoFe_2O_4 are shown in figure 3. The resistive transition exhibits two different regimes. The first is characterized by the normal state that shows a metallic behavior (above $2T_c$ i.e $dp/dT > 0$). The normal state resistivity follows Anderson and Zou relation $\rho_n(T) = A + BT$. Where $\rho_n(T)$ is calculated by using the values of A and B parameters, which are obtained from the linear fitting of resistivity in the temperature range $2T_c$ to 300 K and extrapolated to 0 K gives resistivity slope (dp/dT) and residual resistivity ρ_0 respectively (Figure 3).

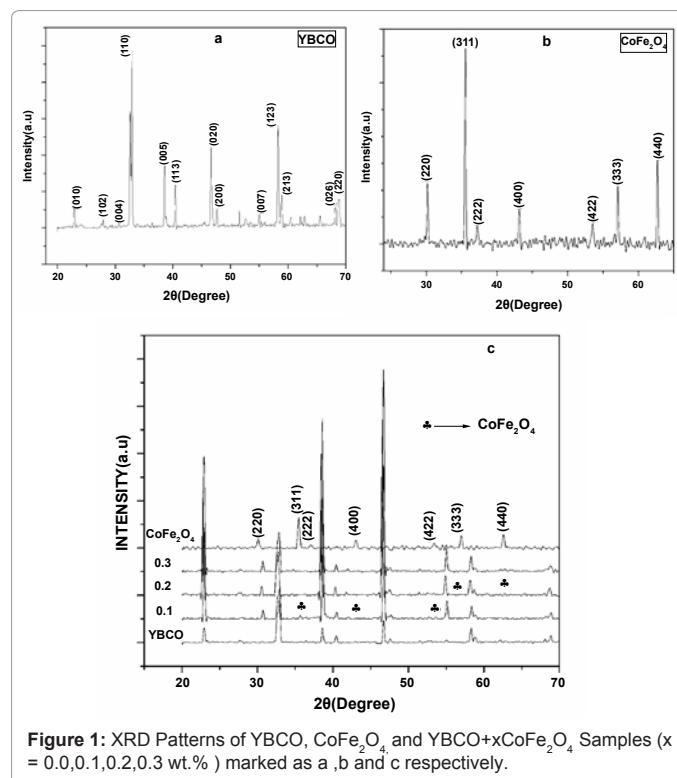
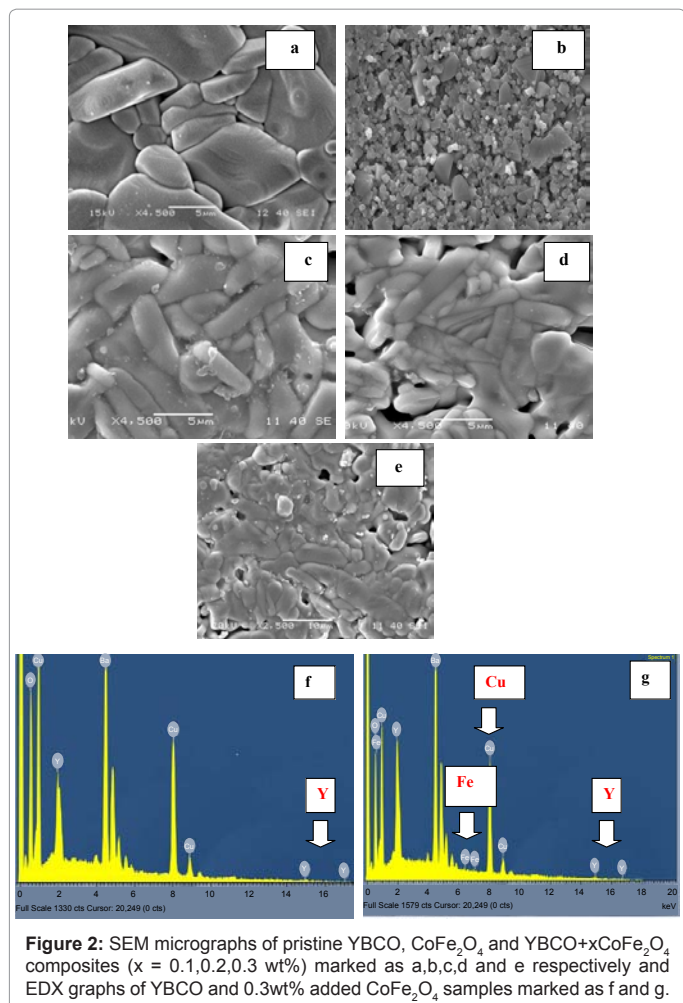


Figure 1: XRD Patterns of YBCO, CoFe_2O_4 , and $\text{YBCO}+x\text{CoFe}_2\text{O}_4$ Samples ($x = 0.0, 0.1, 0.2, 0.3$ wt. %) marked as a, b and c respectively.

CFO(wt%)	a (Å)	b (Å)	c (Å)	V(Å ³)	$\delta = b-a/b+a$	O _{7.5}
0.0	3.815(1)	3.882(1)	11.683(2)	173.023	0.008	6.8
0.1	3.800(2)	3.871(2)	11.655(3)	171.442	0.009	6.9
0.2	3.821(1)	3.888(2)	11.698(3)	173.786	0.008	6.7
0.3	3.820(1)	3.885(1)	11.673(3)	173.235	0.008	6.8

Table 1: Parameters calculated from XRD graphs.

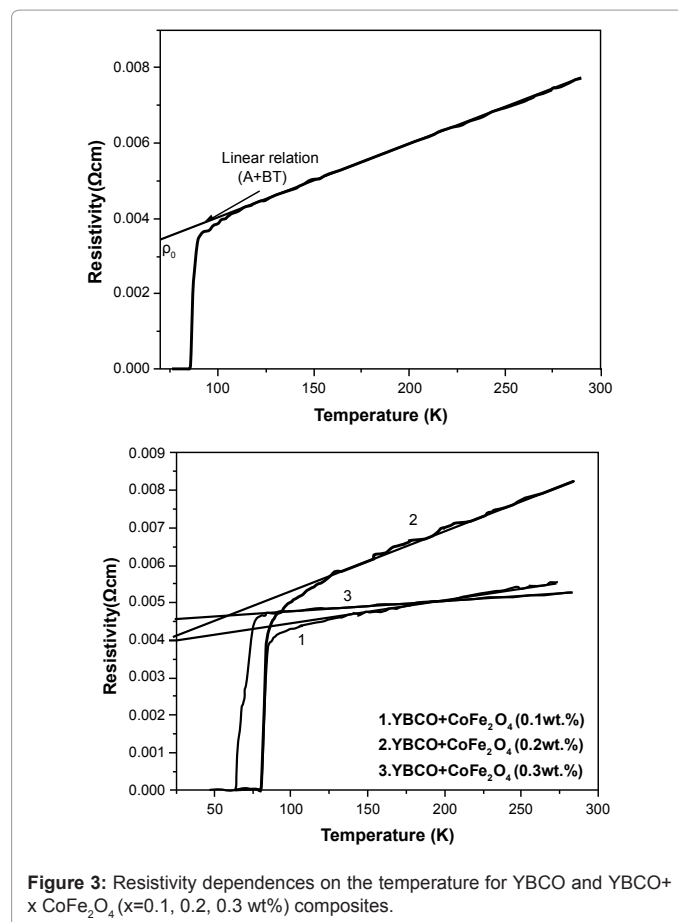


The second is the region characterized by the contribution of Cooper pairs fluctuation to the conductivity below T_c , where $\rho(T)$ is deviating from linearity. This is mainly due to the increasing rate of cooper pair formation on decreasing the temperature. Therefore, the fluctuation induced conductivity in this region follows the AL model to yield the dimensional exponent appropriately to fluctuation-induced conductivity. The normal state resistivity of the composite samples is higher than that of pure sample which is tabulated in table 2. At the temperature value T_{c0} the electrical resistivity vanishes and the phase of the order parameter acquired long range order between the grains of the system. This critical temperature signifies the coherence transition. A finite tailing is observed in the superconducting transition for all the $\text{YBCO}+x\text{CoFe}_2\text{O}_4$ composites before the resistance attains zero value. It indicates that the superconducting grains get progressively coupled to each other by Josephson tunneling across the grain boundary weak links. The zero-resistance at the temperature T_{c0} , characterizes the onset of global superconductivity (where all the grains becomes superconducting i.e. intragrain as well as grain boundaries becomes superconducting) in the samples where the long range superconducting order is achieved. The onset of global resistivity decreases with addition of CFO indicating that it adheres to grain boundary forming weak links.

The absolute resistivity in the normal state may strongly depend on porosity and grain boundaries scattering. It can be seen from figure 3 that there is a decrease of T_c upon the increase of CoFe_2O_4 .

The depression of T_c with CoFe_2O_4 addition may be either due to a decrease in oxygen content in the CuO chains [19] or due to trapping of mobile holes or some mechanism connected with oxygen vacancy disorder [20,21]. The decrease in T_c by further addition of CoFe_2O_4 may be caused by over doping of these particles in the YBCO system, and thus a pair-breaking mechanism may occur at a certain doping level. In this regard, small amount of submicron-sized particle addition improved flux pinning by creating effective pinning centers, while excessive doping retarded the superconductivity of the YBCO system.

The percolation factor ' α_n ' (Table 2) arising due to current frustration caused by misalignment of anisotropic grains and sample defects such as voids and cracks are estimated from the temperature coefficient of resistivity $d\rho/dT$. This factor contributes to percolative conduction in granular copper oxides. Generally in the normal state electrical conduction of granular samples, current path frustration and meandering of current may occur due to two mechanisms. One is associated with the orientational disorder of anisotropic grains [22]. It depends on the degree of texturization, and has its origin in the extreme anisotropy of the copper oxides, the in-plane resistivity ρ_{ab} being orders of magnitude less than the out of plane resistivity ρ_c [23]. Due to the extreme conduction anisotropy, current blocks along the pathways with misaligned grains and current percolates through the sample along unobstructed paths, which results in a cross section reduction and path lengthening [24] that increases resistivity by a multiplicative factor, denote as $1/f$ ($0 < f \leq 1$). Another source of resistivity enhancement comes from structural defects of the grains (i.e. pores, isolating boundaries, microcracks etc.) denoted as $1/\alpha_{str}$ ($0 < \alpha_{str} \leq 1$). Besides the percolative



CFO(wt%)	T_{c0} (K)	T_c (K)	ΔT (K)	$\rho_n(0)$ ($\mu\Omega\cdot\text{cm}$)	α_n	ρ_{wl} ($\mu\Omega\cdot\text{cm}$)	ρ_p ($\mu\Omega\cdot\text{cm}$)	α_{str}
0.0	82.95	85.16	2.21	2090	0.02	41.8	696.66	0.06
0.1	77.27	81.80	4.53	3740	0.07	261.8	1246.66	0.21
0.2	77.41	81.57	4.16	3990	0.03	119.7	1330	0.09
0.3	58.45	64.23	5.78	4500	0.18	810	1500	0.54

Table 2: Variation of normal state and superconducting parameters in the Composites with different CoFe_2O_4 wt%.

processes, a contribution to resistivity coming from the intergrading barriers ρ_{wl} is to be added. So the observed resistivity can be written as,

$$\rho_n = 1/\alpha_n (\rho_{ab} + \rho_{wl}) \quad (1)$$

Where α_n is a shorthand for

$$\alpha_n = f \cdot \alpha_{str} \quad (2)$$

and it may be referred to as the normal-state percolative factor. The normal-state resistivity of polycrystalline HTS is linear with temperature. This linearity of ρ_n enables determination of the two sample parameters α_n and ρ_{wl} . Taking temperature derivatives of equation (1) and assuming ρ_{wl} constant we can get [25,26]

$$\alpha_n = \rho'_{ab} / \rho'_n \quad (3)$$

where the primes stand for temperature derivatives.

Similarly from Eqs. (1) and (3)

$$\rho_{wl} = \rho'_{ab} / \rho'_n \rho_n(0) = \alpha_n \rho_n(0) \quad (4)$$

Where $\rho_n(0)$ is the extrapolation of the normal state resistivity to zero temperature. Based on single crystal measurements ρ_{ab} is assumed [27] to vary linearly with temperature ($\rho'_{ab} = 0.5 \mu\Omega\cdot\text{cm}\cdot\text{K}^{-1}$) with a negligible zero-temperature intercept. For typical polycrystalline Y-based HTS α_n is in the range 0.2–0.05 (Table 2). The main difference between percolation in the normal state and in paracoherent state is that in the latter the orientational disorder is irrelevant as the grain resistivity becomes vanishingly small both in the ab plane and the c direction, resulting in the loss of anisotropy. Once bulk grains go superconducting (but the intergrading junctions remain normal) nothing hinders conduction along that path. Only the structural quality factor α_{str} and the intergrain resistivity ρ_{wl} enter the paracoherent resistivity ρ_p

$$\rho_p = (1/\alpha_{str}) \rho_{wl} \quad (5)$$

From equation (2) and (4)

$$\rho_p = f \rho_n(0) \quad (6)$$

The relation should be $\rho_n(0) > \rho_p > \rho_{wl}$ (Table 2). For YBCO, ρ_p should be equal to approximately one-third of the normal-state resistivity extrapolated to zero temperature [28]. The increasing value of $\rho_n(0)$ and the decreasing trend in the value of zero-resistance critical temperature (T_{c0}) indicates that the connectivity between grains decreases gradually with the addition of composite. All these effects are due to increased inhomogeneities in the intergranular regions. Point defects and chemical dopants may occupy various positions in a real crystal forming substituent or interstitial impurities. Because of the grain boundary is a structurally distorted region in crystals, an extra energy form in the grain boundary region due to the distortion. As a result of the existence of grain boundary energy as well as the Coulomb interaction between the boundaries and the impurity atoms, they tend to attract impurity atoms in order to decrease the grain boundary energy. Therefore, the chemical dopant has a higher probability to stay in the grain boundary region than to stay inside the crystal.

Figure 4 shows the magnetization dependence on the temperature of $\text{YBCO} + x \text{CoFe}_2\text{O}_4$ ($x=0.0, 0.1, 0.2$ wt%) samples. From the M-T graph it is clear that at a mean field transition temperature (T_c) the magnetic lines of force start expelling out of the superconducting specimen. At T_{c0} value they are completely expels out from the sample. This signifies that all the samples show diamagnetic property i.e. satisfying Meissner effect. The magnetization measurement at various temperatures with a field of 500 Gauss showed the compound to be bulk superconducting at 92 K.

Excess conductivity Study

Theoretical background: The Aslamazov-Larkin theory provides the following expression for the excess-conductivity above T_c generated by the thermodynamic fluctuations [5]. It is assumed that the fluctuation conductivity $\Delta\sigma$ diverges as a power-law given by

$$\Delta\sigma = A\epsilon^\lambda \quad (7)$$

$\Delta\sigma$ is defined by

$$\Delta\sigma = (1/\rho - 1/\rho_R) = \sigma - \sigma_R \quad (8)$$

Where ρ and ρ_R are the measured and normal resistivity, $\sigma(T)$ is the measured conductivity and $\sigma_R(T)$ is the extrapolated conductivity under the assumption of a linear behavior of temperature dependent resistivity. The reduced temperature $\epsilon = (T - T_c)/T_c$, defined with respect to the mean field critical temperature (T_c) of the normal to superconducting transition. λ is the Gaussian critical exponent depending on the dimensionality of the HTSC system. The dimensionality D of the fluctuation system is related through the expression,

$$\lambda = 2 - D/2. \quad (9)$$

The effective value of the critical exponent for 3D and 2D are $\lambda = -0.5$ and $\lambda = -1$ respectively [29]. A is a temperature dependent parameter and its values for 3D and 2D are $A = e^2/32\hbar\xi(0)$ and $e^2/16\hbar d$ respectively. ' $\xi(0)$ ' is the zero-temperature coherence length or GL correlation length and 'd' is the effective separation of CuO_2 layers. These relations are based on GL theory and are valid only for the mean field temperature region ($1.01T_c$ to $1.1T_c$). Lawrence and Doniach (LD) extended the AL model for layer superconductors, where conduction occurs mainly in 2D CuO_2 planes and these planes are coupled by Josephson tunneling table 3. The excess conductivity parallel to the layers in the LD Model is given by

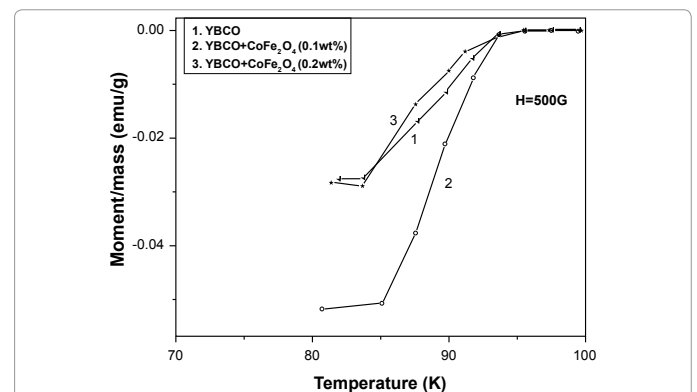


Figure 4: Magnetisation dependences on the temperature of $\text{YBCO} + x \text{CoFe}_2\text{O}_4$ ($x=0.0, 0.1$ & 0.2 wt%).

$$\Delta\sigma(T)_{LD} = e^2/16hde\{1+(2\xi(0)/d)^2 \epsilon^{-1}\}^{-1/2} \quad (10)$$

From equation (10) at temperature close to T_c , $2\xi(0)/d \gg 1$ and $\Delta\sigma(T)$ diverges as $\epsilon^{-1/2}$ which corresponds to 3D behavior. Whereas at $T \gg T_c$, $2\xi(0)/d \ll 1$ and $\Delta\sigma(T)$ diverges as ϵ^{-1} which corresponds to 2D behaviour.

Figure 5 displays the logarithmic plot of excess conductivity as a function of reduced temperature (ϵ). Different regions of the log-log plot were linearly fitted and the exponent values were determined from the slopes to correlate the experimental data with theoretical predicted ones. The plot reveals three distinct regimes i.e. mean-field region or the Gaussian fluctuations, critical fluctuations and short wave fluctuation region.

Gaussian fluctuations: In the mean-field region we represent two fits, one with slope value $\lambda=1.0$ and the other with the value $\lambda=0.5$. The different exponents corresponding to crossover temperatures are as follows, the first exponent is in the normal region at $\log \epsilon$ ($-0.6 \geq \log \epsilon \geq -1$) and its values are close to 1, which indicate that the

Order Parameter Dimensionalities (OPD) are two dimensional (2D). The second exponent is in the critical field region at $\log \epsilon$ ($-1 \geq \log \epsilon \geq -2$) and its values are close to 0.5, which signifies that the OPD are three dimensional (3D). 3D and 2D behavior of superconducting order parameter fluctuation dominates in YBCO composite. The temperature at which dimensionality fluctuation occurs from 3D to 2D is denoted by T_{LD} . T_{LD} values are higher than the T_c values. It reveals that the thermodynamically activated Cooper pairs are generated within the grain at comparatively higher temperatures but due to the intragranular disturbances the mean field critical temperature comes down to lower value. It is possible to infer that this 3D Gaussian regime, determines the spatial limit for the obtainment of long range order of the superconductivity in the material bulk [30]. When the temperature is diminished near T_c , first superconductivity is established in the CuO_2 planes, as a 2D regime, and crosses up to a well defined 3D regime [2].

Critical fluctuations: In superconducting grains Josephson coupling occurs between them. In the absence of magnetic field, their interaction is two dimensional. Considering the Drude like formula for

CoFe ₂ O ₄ (wt.%)	T _G (K)	T _{LD} (K)	T _{2D-SW} (K)
0.0	104.14	128.08	148.63
0.1	104.01	125.45	138.55
0.2	103.24	115.67	127.55
0.3	90.14	104.71	113.95

Table 3: CoFe₂O₄ content dependence of different cross over temperatures (Ginzburg-Landau, Lawrence-Doniach and Shortwave fluctuation).

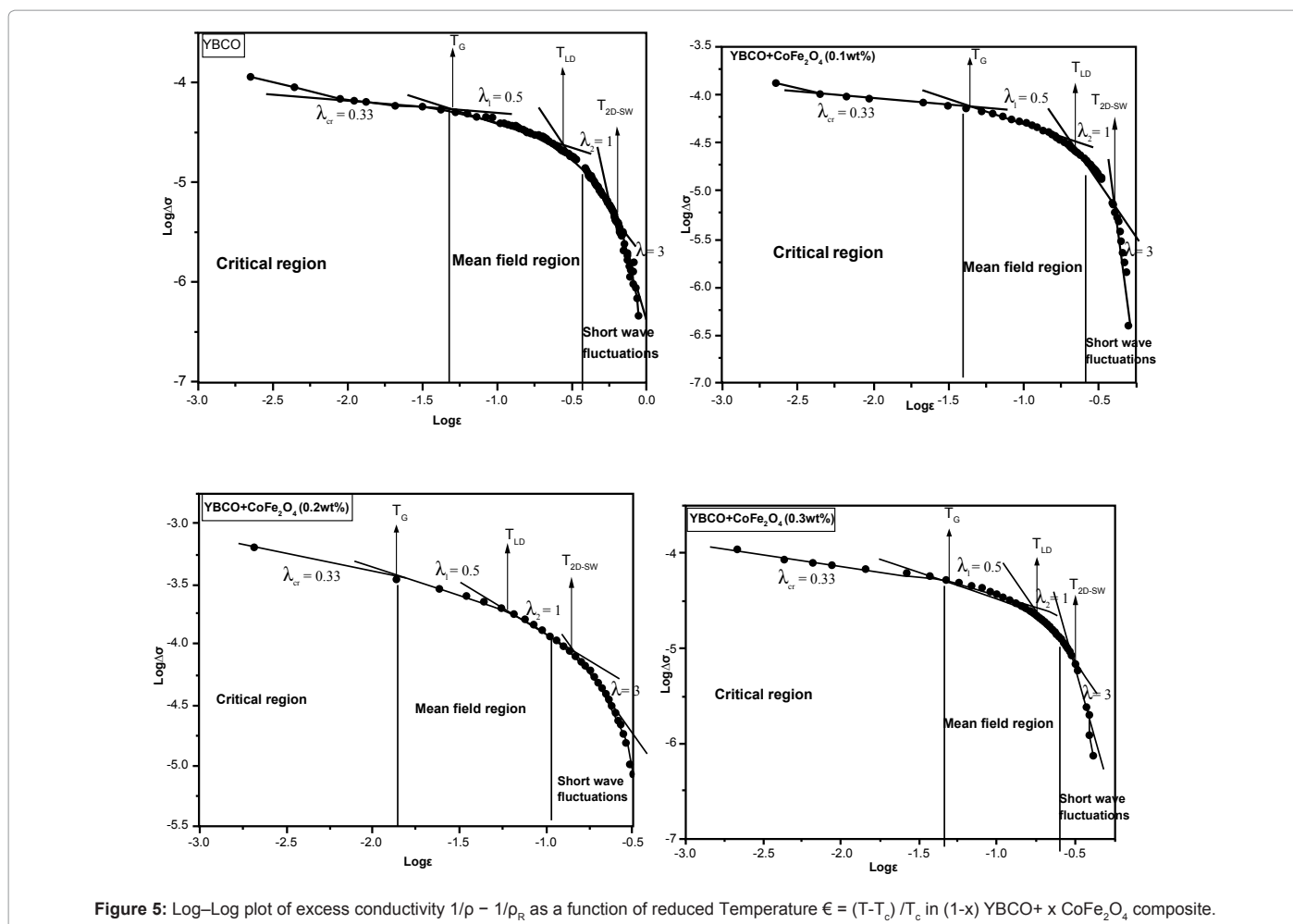


Figure 5: Log-Log plot of excess conductivity $1/\rho - 1/\rho_R$ as a function of reduced Temperature $\epsilon = (T-T_c)/T_c$ in $(1-x)\text{YBCO} + x\text{CoFe}_2\text{O}_4$ composite.

excess conductivity and dynamical scaling theory for coherence length, the critical exponent of excess conductivity is obtained [31,32]

$$\lambda_{cr} = \nu (2-D - \eta + z) \quad (11)$$

Where z is the dynamical exponent, η is the exponent of the order parameter correlation function, D is the dimensionality of the fluctuations and ν is the critical exponent for the coherence length. Using this relation for the fluctuation conductivity data in the critical region, one can estimate the dynamical exponent z [33]. According to renormalization group calculations, $\nu=0.67$ and $\eta=0.03$ are expected and $z=0.32$ being predicted by the theory of dynamical critical scaling [34]. Using this values with $D=3$ yields $\lambda_{cr}=0.33$ which is called as the 3D-XY-E because of the model-E dynamics [35]. The critical fluctuation and 3D fluctuation regions intersect at temperature T_G . Still closer to T_G , a critical scaling regime beyond 3D-XY is observed, labeled by the exponent $\lambda_{cr}=0.16$ [36-38]. The regime beyond 3D-XY with $\lambda_{cr}=0.17$ was first observed in YBCO single crystal [39]. This exponent is known to characterize the critical resistive transition in classical granular arrays formed by metallic superconducting particles embedded in a poorly conducting matrix.

Shortwave Fluctuations

The excess conductivity varies sharply with exponent $\lambda=3$ with $\log \epsilon$ ($-0.5 \geq \log \epsilon \geq -0.1$) which highlights the presence of short wave fluctuations. The crossover temperature from 2D to short wave fluctuations (T_{2D-SW}) is indicated in table 1. Short-wavelength fluctuations (SWF) effect appears when the characteristic wavelength of the order parameter becomes of the order of coherence length [40].

From the data of table 1 it is clear that with an increase in wt% of CoFe_2O_4 in YBCO the mean field transition temperature T_c and T_{c0} decreases gradually. The different crossover temperatures T_G , T_{LD} and T_{2D-SW} also decrease with an increase in wt%. The transition width $\Delta T = T_c - T_{c0}$ increases with increasing CoFe_2O_4 content.

Conclusion

The effect of ferromagnetic inhomogeneity of CoFe_2O_4 on the structural and fluctuation conductivity is systematically studied. The different regions observed are the critical region at $T < T_c$, the mean field region at T close to T_c and the short wave fluctuations at $T > T_c$. The experimental data fit with theoretical predicted ones. Decrease in T_{LD} in the composite, indicates the dominating nature of fluctuation of Cooper pairs in 3D. The large T_c degradation may be due to the redistribution of charges in the superconducting system due to oxygen content, and the resistance of the weak link caused by inhomogeneities. Variation of lattice parameters and crystallite volume indicates the incorporation of iron into the superconducting grains. The ferromagnetic inclusion reduces the grain size and increase the strength and hardness of the parent compound.

Acknowledgments

The authors gratefully acknowledge the Department of Science and Technology, Govt. of India for providing fellowship to carry out this work. The authors would like to thank Dr. A. Mitra, National Metallurgical Laboratory, Jamshedpur, for providing facility for M-T measurement.

References

- Aswal DK, Singh A, Sen S, Kaur M, Viswandham CS, et al. (2002) Effect of grain boundaries on paraconductivity of $\text{YBa}_2\text{Cu}_3\text{O}_x$. J Phys Chem Solids 63: 1797-1803.
- Kujur A, Behera D (2012) DC electrical resistivity and magnetic studies in Yttrium Barium Copper oxide/barium titanate composite thin films. Thin Solid Films 520: 2195-2199.

- Kuriyama T, Urata M, Yazawa T, Yamamoto K, Ohtani Y et al. (1994) Cryocooler Directly Cooled 6 T Nbt Superconducting Magnet System With 180-Mm Room-Temperature Bore. Cryogenics 34: 643-646.
- Foltyn SR, Civale L, MacManus-Driscoll JL, Jia QX, Maiorov B, et al. (2007) Materials science challenges for high-temperature superconducting wire. Nature Materials 6: 631-642.
- Aslamazov LG, Larkin AI (1968) Effect of Fluctuations on the Properties of a Superconductor above the Critical Temperature. Sov Phys Solid State 10: 1104-1111.
- Kanda E (1971) Proceedings of the 12th International Conference on Low Temperature Physics. Academic Press of Japan, Japan.
- Blatter G, Feigel'man MV, Geshkenbein VB, Larkin AI, Vinokur VM (1994) Vortices in high-temperature superconductors. Rev Mod Phys 66: 1125-1388.
- Ikeda R, Ohmi T, Tsuneto T (1991) Comment on "Giant out-of-plane magnetoresistance in Bi-Sr-Ca-Cu-O: A new dissipation mechanism in copper-oxide superconductors?". Phys Rev Lett 67: 3874-3874.
- Zhao Y, Cheng CH, Wang JS (2005) Flux pinning by NiO-induced nano-pinning centres in melt-textured YBCO superconductor. Supercond Sci Tech 18: S43.
- Campbell TA, Haugan TJ, Maartense I, Murphy J, Brunke L, et al. (2005) Flux pinning effects of Y_2O_3 nanoparticulate dispersions in multilayered YBCO thin films. Physica C: Superconductivity 423: 1-18.
- He ZH, Habisreuther T, Bruchlos G, Litzkendorf D, Gawalek W (2001) Investigation of microstructure of textured YBCO with addition of nanopowder SnO_2 . Physica C: Superconductivity 356: 277-284.
- Yang ZQ, Su XD, Qiao GW, Guo YC, Dou SX, et al. (1999) Flux-pinning enhancement in Ag-sheathed Bi-2223 tapes by nanometer-SiC addition. Physica C: Superconductivity 325: 136-142.
- Albiss BA, Al-Rawashdeh N, Jabal AA, Gharaibeh M, Obaidat IM, et al. (2010) Polycrystalline $\text{YBa}_2\text{Cu}_3\text{O}_{7-x}$ with Nano-sized Al_2O_3 Inclusions. J Supercond Nov Magn 23: 1333-1340.
- Wang J, Chen-Fong T, Zhenxing B, Donald NG, Wang H (2009) Microstructural and Pinning Properties of $\text{YBa}_2\text{Cu}_3\text{O}_{7-x}$ Thin Films Doped With Magnetic Nanoparticles. IEEE T Appl Supercon 19: 3503-3506.
- Kulpa A, Chaklader ACD, Osborne NR, Roemer G, Sullivan B, et al. (1989) Influence of oxygen ordering and sintering temperatures on the superconducting transition temperature of $\text{YBa}_2\text{Cu}_3\text{O}_x$ compound at fixed oxygen content x higher than $x=6.8$. Solid State Commun 71: 265-268.
- Kurihara S (1989) Interacting hole-spin model for oxide superconductors: NMR relaxation rate. Physica C: Superconductivity 164: 1505-1506.
- Benzi P, Bottizzo E, Rizzi N (2004) Oxygen determination from cell dimensions in YBCO superconductors. J Cryst Growth 269: 625-629.
- Wimbush SC, Durrell JH, Tsai CF, Wang H, Jia QX, et al. (2010) Enhanced critical current in $\text{YBa}_2\text{Cu}_3\text{O}_{7-x}$ thin films through pinning by ferromagnetic YFeO_3 nanoparticles. Supercond Sci Technol 23: 045019.
- Brecht E, Schmahl WW, Miede G, Rodewald M, Fuess H, et al. (1996) Thermal treatment of $\text{YBa}_2\text{Cu}_3-x\text{AlxO}_{6.5}$ single crystals in different atmospheres and neutron-diffraction study of excess oxygen pinned by the Al substituents. Physica C: Superconductivity 265: 53-66.
- Zhang J, Liu F, Cheng G, Shang J, Liu J, et al. (1995) Electron structure and vacancy properties and Al-substitution dependence of the positron lifetime in $\text{Y}_1-x\text{Ca}_x\text{Ba}_2\text{Cu}_3\text{O}_{7-x}$ superconducting ceramics. Phys Lett A 201: 70-76.
- Awana VPS, Malik SK, Yelon WB, Cardoso CA, DeLima OF, et al. (2000) Neutron diffraction on $\text{Er}_{1-x}\text{Ca}_x\text{Ba}_2\text{Cu}_3\text{O}_{7-x}$ ($0.0 \leq x \leq 0.3$) system: possible oxygen vacancies in Cu-O₂ planes. Physica C: Superconductivity 338: 197-204.
- Ekin JW, Braginski AI, Panson AJ, Janock MA, Capone DW, et al. (1987) Evidence for weak link and anisotropy limitations on the transport critical current in bulk polycrystalline $\text{Y}_1\text{Ba}_2\text{Cu}_3\text{O}_x$. J Appl Phys 62: 4821-4828.
- Friedmann TA, Rabin MW, Giapintzakis J, Rice JP, Ginsberg DM (1990) Direct measurement of the anisotropy of the resistivity in the a-b plane of twin-free, single-crystal, superconducting $\text{YBa}_2\text{Cu}_3\text{O}_{7-x}$. Phys Rev B 42: 6217-6221.
- Halbritter J (1989) Percolation in Superconducting Cuprates: Resistivity and Critical Currents. Int J Mod Phys B 3: 719-732.
- Bungre SS, Meisels R, Shen ZX, Caplin AD (1989) Are classical weak-link

- models adequate to explain the current-voltage characteristics in bulk $\text{YBa}_2\text{Cu}_3\text{O}_7$. Nature 341: 725-727.
26. Babic E, Prester M, Marohnic Z, Car T, Biskup N, et al. (1989) Critical currents and differential resistance of $\text{YBa}_2\text{Cu}_3\text{O}_{7-x}$ superconducting ceramics. Solid State Commun 72: 753-757.
27. Batlogg B (1992) Physics of High-Temperature Superconductors. Springer-Verlag Berlin 219.
28. Diaz A, Maza J, Vidal F (1997) Anisotropy and structural-defect contributions to percolative conduction in granular copper oxide superconductors. Phys Rev B 55: 1209-1215.
29. Tang XG, Liu QX, Wang J, Chan HLW (2009) Electric-field dependence of dielectric properties of sol-gel derived $\text{Ba}(\text{Zr}_{0.2}\text{Ti}_{0.8})\text{O}_3$ ceramics. Appl Phys A 96: 945-952.
30. Roa-Rojas J, Tellez DAL, Sarmiento MPR (2006) Pairing and coherence transition in $\text{La}_{1.82}\text{Sr}_{0.18}\text{CuO}_4$ strongly two-dimensional superconductor. Braz J Phys 36: 1105-1108.
31. Vieira VN, Pureur P, Schaf J (2002) Effects of Zn and Mg in Cu sites of $\text{YBa}_2\text{Cu}_3\text{O}_{7.5}$ single crystals on the resistive transition, fluctuation conductivity, and magnetic irreversibilities. Phys Rev B 66: 224506-224517.
32. Esmaeili A, Sedghi H, Amniat-Talab M, Talebian M (2011) Fluctuation-induced conductivity and dimensionality in the new Y-based $\text{Y}_3\text{Ba}_5\text{Cu}_8\text{O}_{18-x}$ superconductor. Eur Phys J B 79: 443-447.
33. Rosenblatt J, Peyral P, Raboutou A, Lebeau C (1988) Coherence in 3D networks: Application to high- T_c superconductors. Physica B: Condensed Matter 152: 95-99.
34. Le Guillou JC, Zinn-Justin J (1980) Critical exponents from field theory. Phys Rev B 21: 3976-3998.
35. Hohenberg PC, Halperin BI (1977) Theory of dynamic critical phenomena. Rev Mod Phys 49: 435-479.
36. Jurelo AR, Menegotto Costa R, de Andrade AVC, Junior PR, da Cruz GK, et al. (2009) Analysis of fluctuation conductivity of polycrystalline $\text{Er}_{1-x}\text{Pr}_x\text{Ba}_2\text{Cu}_3\text{O}_{7.5}$ superconductors. Braz J Phys 39: 667-672.
37. Jurelo AR, Junior PR, Carrillo AE, Puig T, Obradors X, et al. (2003) Fluctuation conductivity in melt-textured $\text{REBa}_2\text{Cu}_3\text{O}_{7-d}$ superconductors. Phys C 399: 87-92.
38. Annapurna M, Dhruvananda B (2010) Fluctuation induced magneto-conductivity studies in $\text{YBa}_2\text{Cu}_3\text{O}_{7-d}+x\text{BaZrO}_3$ composite high T_c superconductors. Physica C 470: 295-303.
39. Costa RM, Pureur P, Gusmao M, MGS Senoussi, Behnia K (2000) Scaling beyond 3D XY in the fluctuation conductivity of $\text{YBa}_2\text{Cu}_3\text{O}_{7-d}$. Solid State Commun 113: 23-27.
40. Harabor A, Harabor NA, Deletter M (2006) Short-wavelength fluctuation regime in paraconductivity of bulk monophasic (Bi, Pb)-2223 superconductor system. J Optoelectron Adv M 8: 1072-1076.